Gamma protocadherins are required for synaptic development in the spinal cord

Joshua A. Weiner*†‡, Xiaozhong Wang‡§, Juan Carlos Tapia*¶, and Joshua R. Sanes*¶‖

*Department of Anatomy and Neurobiology, Washington University Medical School, 660 South Euclid Avenue, St. Louis, MO 63110; †Department of Biological Sciences, University of Iowa, 143 Biology Building, Iowa City, IA 52242; §Department of Biochemistry, Molecular Biology, and Cell Biology, Northwestern University, Evanston, IL 60208-3500; and ¶Department of Molecular and Cellular Biology, Harvard University, 7 Divinity Avenue, Cambridge, MA 02138

This contribution is part of the special series of Inaugural Articles by members of the National Academy of Sciences elected on April 30, 2002.

Contributed by Joshua R. Sanes, October 25, 2004

Fifty-eight cadherin-related protocadherin (*Pcdh*) genes are tandemly arrayed in three clusters (α, β, and γ) on mouse chromosome 18. The large number of clustered *Pcdh* family members, their presence at synapses, and the known binding specificities of other cadherin superfamily members all suggest that these Pcdhs play roles in specifying synaptic connectivity. Consistent with this idea, mice lacking all 22 genes of the *Pcdh*-γ cluster have decreased numbers of spinal cord synapses and are nearly immobile. Interpretation of this phenotype was complicated, however, by the fact that *Pcdh*-γ loss also led to apoptosis of many spinal interneurons. Here, we used two methods to circumvent apoptosis and neurodegeneration in *Pcdh*-γ mutant mice. First, we analyzed mutants lacking both Pcdh-γ proteins and the proapoptotic protein Bax. Second, we generated a hypomorphic allele of *Pcdh*-γ in which apoptosis was minimal. In both cases, spinal interneurons were preserved but the mice bore dramatically decreased numbers of spinal cord synapses and exhibited profound neurological defects. Moreover, synaptic function was compromised in neurons cultured from the hypomorphs. These results provide evidence for a direct role of γ-Pcdhs in synaptic development and establish genetic tools for elucidating their contribution to synaptic specificity.

synaptogenesis | Bax | interneuron

As synapses form, their presynaptic and postsynaptic elements become linked by transmembrane adhesion molecules, including members of the Ig and cadherin superfamilies. Some of these adhesion molecules, such as SynCAM, neuroligin, and neurexin, might function primarily to coordinate presynaptic and postsynaptic differentiation, whereas others might contribute to the selectivity with which synaptic connections form between appropriate partners (reviewed in refs. 1–4). The diversity of the Ig and cadherin families and the binding specificities of individual members suggests that they might be involved in both aspects of synaptogenesis. Support for roles in synaptic specificity has recently been obtained for at least five Ig superfamily members, Sidekick-1 and-2 in vertebrates (5), Syg-1 and -2 in worms (6, 7), and DS-CAM in flies (8, 9).

Additional attractive candidate synaptic recognition molecules are the nearly 60 cadherin-related protocadherin (Pcdh) genes tandemly arrayed in three clusters on a single chromosome in mammals (10, 11). These clusters, termed *Pcdh*-α, -β, and -γ, each contain multiple "variable" exons encoding the extracellular, transmembrane, and proximal cytoplasmic domains of individual isoforms. Within the *Pcdh*-α and -γ clusters, each variable exon is transcribed from its own promoter and spliced to "constant" exons that encode a shared C-terminal domain (12–15). Many neuronal populations express multiple *Pcdh* genes, and the α- and γ-Pcdh proteins are concentrated at, although not exclusively localized to, synapses (16–19). Together, these features have led to the hypothesis that combinatorial patterns of Pcdh expression promote specific interactions between presynaptic and postsynaptic partners (20–22).

In an attempt to test this hypothesis, we generated and analyzed mice from which the entire *Pcdh*-γ locus had been deleted (*Pcdh*-$\gamma^{del/del}$; ref. 17). The number of synapses in the gray matter of the spinal cord was decreased in these mice, consistent with the idea that γ-Pcdhs are required for synaptic development. However, the interpretation was complicated because *Pcdh*-γ deletion also led to apoptosis of spinal interneurons. Thus, the reduction in synapse number might have been either a direct consequence of *Pcdh*-γ deletion or an indirect consequence of neurodegeneration.

We have now used two methods to distinguish these alternatives. First, we prevented apoptosis in *Pcdh*-$\gamma^{del/del}$ mice by removal of the proapoptotic Bcl-2 family member Bax. *Bax*$^{-/-}$ mice are outwardly normal and live to adulthood (23). However, naturally occurring apoptosis of many neuronal populations is greatly decreased in these mutants (24–26), making them useful for examining characteristics of neurons that would otherwise die (27, 28). Second, we generated a hypomorphic allele of the *Pcdh*-γ locus (*Pcdh*-γ^{tr}). *Pcdh*-$\gamma^{tr/tr}$ mice, like *Pcdh*-$\gamma^{del/del}$ mice, die shortly after birth. Unexpectedly, however, neuronal apoptosis was not substantially elevated in *Pcdh*-$\gamma^{tr/tr}$ mice. Thus, we were able to use both *Pcdh*-$\gamma^{del/del}$;*Bax*$^{-/-}$ and *Pcdh*-$\gamma^{tr/tr}$ mutants to examine spinal neuron synapses in the absence of neurodegeneration. Our morphological and electrophysiological results support a direct role for γ-Pcdhs in synaptic development.

Materials and Methods

Mouse Strains. Mice lacking the entire 22-gene *Pcdh*-γ locus (*Pcdh*-$\gamma^{del/del}$; ref. 17) and mice lacking *Bax* (23, 24) have been described. Both were maintained on a C57/B6 background. The targeting vector for the C-terminal truncation allele (*Pcdh*-γ^{tr}) consisted of a *Not*I/*Sal*I-digested, 6.4-kb 5′ homology arm generated by PCR, an internal ribosome entry site (IRES), a GFP-β-galactosidase (LacZ) fusion gene, a loxP-flanked neomycin resistance gene for positive selection, an *Nhe*I/*Eco*RI-digested, 1.6-kb 3′ homology arm amplified by PCR, and a thymidine kinase-negative selection marker. Homologous recombination led to the insertion of the IRES-GFP-LacZ cassette into constant exon 3, resulting in truncation of γ-Pcdh proteins 57 aa from the C terminus. Targeted ES clones were identified by PCR, and the selection marker was excised by transient expression of Cre recombinase in ES cells before blastocyst injection.

Abbreviations: Pcdh, protocadherin; MAP2, microtubule-associated protein 2; GAD, glutamic acid decarboxylase; VGlut, vesicular glutamate transporter; PSD, postsynaptic density.

See accompanying Biography on page 5.

‡J.A.W. and X.W. contributed equally to this work.

‖To whom correspondence should be addressed. E-mail: sanesj@mcb.harvard.edu.

www.pnas.org/cgi/doi/10.1073/pnas.0407931101

Immunofluorescence. Tissues were frozen unfixed or after immersion in 4% paraformaldehyde and cryoprotection in 30% sucrose. Cryostat sections were cut at 10–15 μm, and sections from unfixed blocks were fixed in 100% methanol for 10 min at −20°C. Sections were blocked in 2.5% BSA and 0.1% Triton X-100 in PBS for 1 h, followed by incubation with primary antibody at 4°C overnight in the same solution. Sections were washed in PBS and secondary antibodies (Alexa Fluor 488- or 568-conjugated) applied in PBS for 1 h. Nuclei were counterstained with 4′,6-diamidino-2-phenylindole added to the final wash.

Antibodies used (and their sources) were: anti-NeuN (Chemicon); anti-gephyrin and anti-glycine receptor (Alexis, San Diego); anti-microtubule-associated protein 2 (MAP2, Sigma); anti-class III β-tubulin (TuJ1, Covance, Princeton, NJ); anti-glutamic acid decarboxylase (GAD, Developmental Studies Hybridoma Bank, Iowa City, IA); anti-vesicular glutamate transporter (VGlut) 1 and 2 (mixed 1:1 and used together, Chemicon); anti-postsynaptic density (PSD)-95 (Affinity Bioreagents, Golden, CO); anti-synaptophysin (Zymed); anti-cleaved caspase-3 (Cell Signaling Technology, Beverly, MA); anti-neurofilaments (Sternberger–Meyer, Jarrettsville, MD); rabbit anti-GFP (Chemicon); and a rabbit antiserum to the common *Pcdh-γ* C-terminal exons (17). Neuro Trace 435 (Molecular Probes) was used as a fluorescent Nissl stain.

For quantification of synapse and neuron number, digital micrographs of control and mutant spinal cord sections or neuronal cultures were taken at equivalent locations and camera exposures by using ×63 or ×100 oil objectives on a Zeiss Axioplan microscope. These digital images were adjusted and thresholded similarly in METAMORPH (Universal Imaging, Downingtown, PA), and synaptic puncta were counted by using automated analysis functions. NeuN+ neurons were counted manually. Statistical significance was determined by using multifactorial ANOVA and Fisher's probable least-squares difference post hoc tests calculated with STATVIEW software (Abacus Concepts, Berkeley, CA).

Spinal Neuron Cultures. Spinal neurons were cultured by methods modified from ref. 29. Spinal cords were removed from embryonic day 13 control and *Pcdh-γ*$^{tr/tr}$ embryos in 135 mM NaCl, 5 mM KCl, 75 mM Na_2HPO_4, 0.2 mM KH_2PO_4, 20 mM glucose, 44 mM sucrose, and 10 mM Hepes. Extra-neural tissue was taken from each embryo for genotyping. Each spinal cord was transferred to a well of a 12-well tissue-culture dish (Nunc) containing 1 ml of trypsin-EDTA (0.05% trypsin), cut into small pieces with spring scissors, incubated at 37°C and 5% CO_2 for 30 min, diluted with 2 ml of plating medium (DMEM plus 10% FCS, 10% horse serum, and penicillin/streptomycin) to inhibit trypsin, transferred to 1 ml fresh medium, and triturated 10–20 times with a fire-polished Pasteur pipet. Cells were then plated on 13-mm glass coverslips that had been coated sequentially with poly-L-lysine and laminin-1 (400,000–500,000 cells per well) and placed at 37°C and 5% CO_2. After 24 h, the medium was changed to growth medium [DMEM plus 10% FCS and N2 supplements (Gibco)] without antibiotics. Growth medium was changed every 2–3 days. Cultures were used for electrophysiological recordings at 8–11 days *in vitro* (DIV) or fixed for immunofluorescence at 9 DIV. Cultures consisted of a "lawn" of glial fibrillary acidic protein-positive astrocytes on which clusters of interneurons grew. Motor neurons did not survive the plating procedure and were completely absent. A few dorsal root ganglia sensory neurons were present in some cultures, but they were easily distinguishable from interneurons by their large somata and expression of neurofilaments and were excluded from histological and electrophysiological analyses.

Western Blotting. We generated full-length or C-terminally truncated Pcdh-γ-EGFP fusion proteins by PCR from a cDNA clone encoding the full-length Pcdh-γ C4 isoform. PCR products were cloned into an EGFP-containing vector to generate in-frame fusions, which were then transferred to the expression vector pcDNA3 (Invitrogen). The full-length fusion protein corresponds to that produced by the *Pcdh-γ*^{fusg} allele reported previously (17), and the truncated protein corresponds to that generated in the *Pcdh-γ*^{tr} allele. Both the full-length and truncated constructs were transfected into COS-7 cells, and the recombinant proteins were analyzed by Western blotting using standard methods.

Electrophysiological Recordings. Current- and voltage-clamp recordings were performed as described (30). Data files obtained with AXOSCOPE 9.0 were analyzed offline with MINIANALYSIS 5.0 software to obtain peak amplitudes, frequencies, and decay time constants. The decay phases of inhibitory and excitatory postsyn-

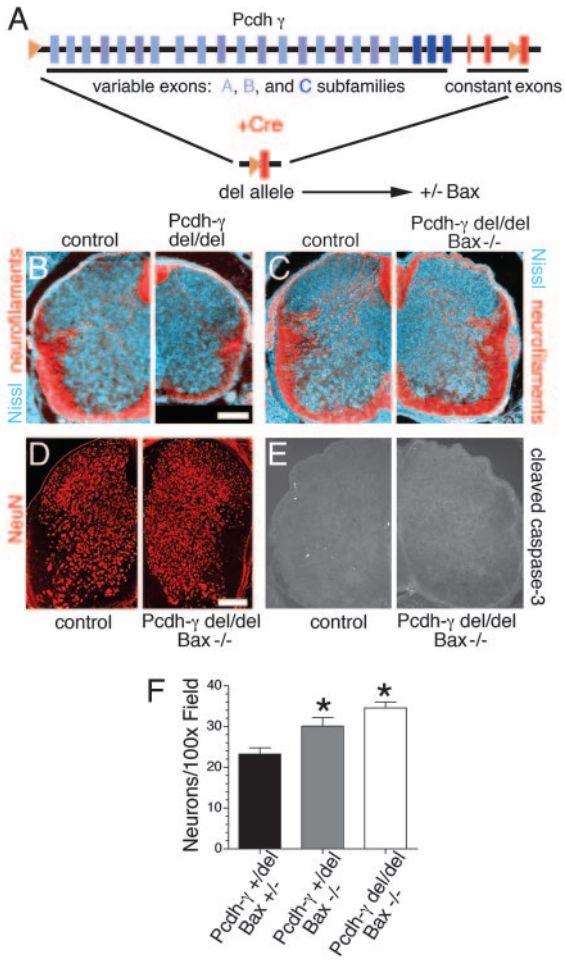

Fig. 1. Loss of *Bax* rescues spinal interneuron apoptosis in *Pcdh-γ* deletion mice. (*A*) Schematic of the targeted *Pcdh-γ* genomic locus with loxP sites (orange triangles) upstream of the first variable exon and within constant exon 3. The locus was deleted by transfection of Cre to generate the *Pcdh-γ*^{del} allele. This line was crossed with *Bax* mice to produce *Pcdh-γ*$^{del/del}$;*Bax*$^{-/-}$ double mutants. (*B–E*) In contrast to *Pcdh-γ*$^{del/del}$ single mutants (*B*), which exhibit spinal cord hypoplasia caused by apoptosis of interneurons and loss of axonal tracts (stained for neurofilaments, red), double mutant neonates are morphologically normal (*C*), exhibit no loss of interneurons (*D*; neurons stained for NeuN), and lack evidence of apoptosis (*E*; staining for cleaved caspase-3). (*F*) Neuron number is increased in *Bax*$^{-/-}$ mice, because apoptosis is blocked; the *Pcdh-γ* mutation has no significant effect on neuron number in this background. Bars show mean ± SEM of 7–14 microscope fields from three animals per genotype. *, $P < 0.02$, compared to *Pcdh-γ*$^{+/del}$;*Bax*$^{+/-}$. (Bar: 100 μm.)

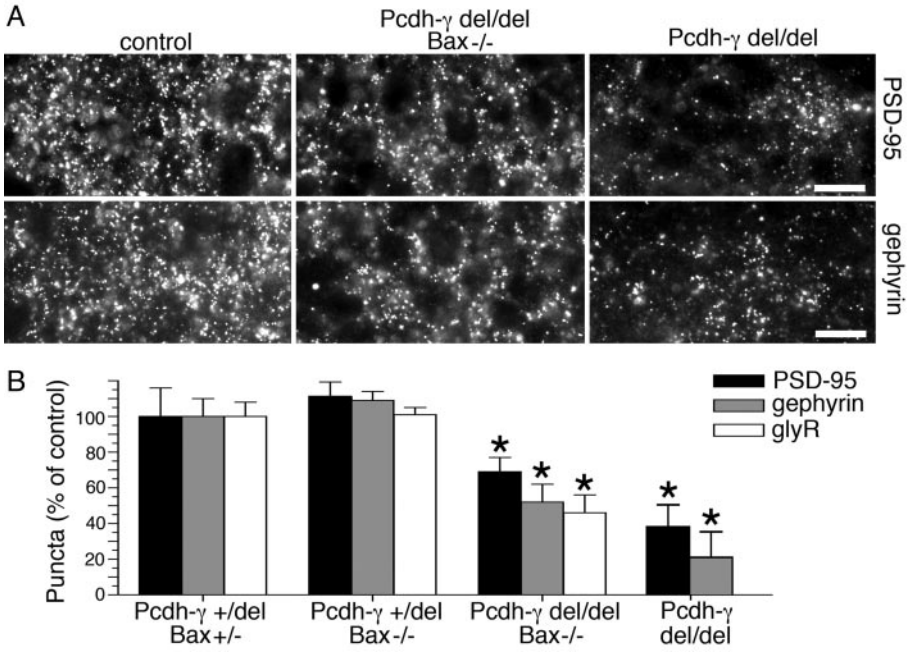

Fig. 2. Reduced synaptic density in the absence of neurodegeneration in *Pcdh*-$\gamma^{del/del}$;$Bax^{-/-}$ double mutant spinal cord. (*A*) Immunostained synaptic puncta in sections through the intermediate gray of control, *Pcdh*-$\gamma^{del/del}$ and *Pcdh*-$\gamma^{del/del}$;$Bax^{-/-}$ neonatal spinal cords. (Bars: 12 μm.) (*B*) Both *Pcdh*-$\gamma^{del/del}$ and *Pcdh*-$\gamma^{del/del}$;$Bax^{-/-}$ mutants exhibit significant reductions in the density of excitatory (anti-PSD-95+) and inhibitory [anti-gephyrin+ and anti-glycine receptor+ (glyR+)] synapses. Bars show mean ± SEM of 7–14 microscope fields from three animals per genotype and are expressed as percent of control (*Pcdh*-$\gamma^{+/del}$;$Bax^{+/-}$). *, $P < 0.05$. Data from *Pcdh*-$\gamma^{del/del}$ single mutants, recalculated from data in Wang *et al.* (17), are shown for comparison.

aptic currents were best-fitted with a single exponential curve. Data are expressed as mean ± SEM. Statistical comparisons were performed by using Student's *t* test, ANOVA, or the Kolmogorov–Smirnov test.

Results

Synaptic Defects in Pcdh-γ/BAX Double Mutants. As reported previously, spinal cords of *Pcdh*-$\gamma^{del/del}$ mice were hypoplastic and exhibited high levels of interneuronal apoptosis and neurogeneration (ref. 17 and Fig. 1 *A* and *B*). These defects made it impossible to determine whether decreased synapse number in the *Pcdh*-$\gamma^{del/del}$ spinal cord reflected a role for γ-Pcdhs in synaptogenesis or a consequence of neurodegeneration. To distinguish these alternatives, we attempted to block neuronal apoptosis by mating *Pcdh*-γ^{del} mice to mice harboring a null allele of the proapoptotic gene *Bax* (23). Because *Pcdh*-$\gamma^{del/del}$

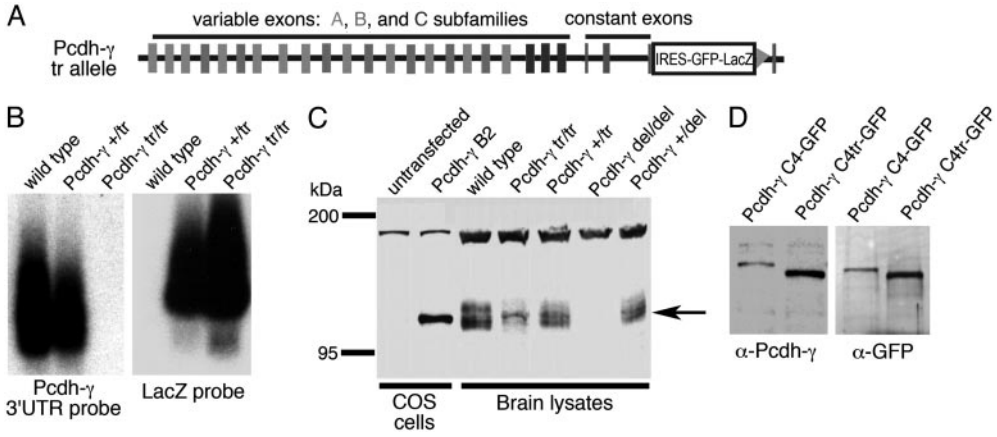

Fig. 3. A hypomorphic, C-terminally truncated allele of *Pcdh*-γ (*Pcdh*-γ^{tr}). (*A*) The targeted *Pcdh*-γ^{tr} allele contains an internal ribosome entry site (IRES)-GFP/LacZ fusion cassette inserted into constant exon 3, followed by a loxP site (triangle) left behind by excision of a neo selection marker. Cassette insertion results in a 57-aa truncation of the common *Pcdh*-γ C terminus. (*B*) Duplicate Northern blots of brain RNA hybridized with probes against the *Pcdh*-γ constant exon 3′ UTR and the *LacZ* gene. In *Pcdh*-$\gamma^{tr/tr}$ mice, transcription of the inserted cassette is observed in place of the *Pcdh*-γ 3′ UTR. (*C*) Western blots of lysates from brains of WT and *Pcdh*-γ^{tr} or *Pcdh*-γ^{del} mice probed with a rabbit antiserum against the *Pcdh*-γ common C terminus. Levels of γ-Pcdh proteins (arrow) are reduced in *Pcdh*-$\gamma^{tr/tr}$ brains. Specificity of the antiserum is demonstrated by its recognition of recombinant protein in lysates of COS cells transfected with a full-length *Pcdh*-γB2 cDNA and by the absence of the appropriate band in *Pcdh*-$\gamma^{del/del}$ brains. The upper band is nonspecific. (*D*) Duplicate Western blots of lysates from COS cells transiently transfected with constructs encoding either full-length or C-terminally truncated *Pcdh*-γ C4/GFP fusion proteins, probed with anti-*Pcdh*-γ and anti-GFP antisera. Similarity of the two blots suggests that C-terminally truncated protein retains major anti-*Pcdh*-γ epitopes. Difference in intensity between lanes within each blot is caused by a difference in the number of transfected cells between cultures.

mice die at birth (17) and $Bax^{-/-}$ mice are infertile (23), we first generated compound heterozygotes, which were then mated to obtain $Pcdh\text{-}\gamma^{del/del}$;$Bax^{-/-}$ double mutants at the expected frequency of ≈1/16.

Double mutant spinal cords were grossly normal in size, shape, and organization (Fig. 1*C*), had a normal density of neuronal somata (stained with antibodies to NeuN; Fig. 1 *D* and *F*) and fiber tracts (stained with antibodies to neurofilaments; Fig. 1*C*), and exhibited few, if any, apoptotic cells (stained with antibodies to activated caspase-3; Fig. 1*E*). Thus, deletion of *Bax* effectively prevented the apoptosis, neurodegeneration, and spinal cord hypoplasia caused by *Pcdh-γ* deletion. Nonetheless, $Pcdh\text{-}\gamma^{del/del}$;$Bax^{-/-}$ double mutants, like $Pcdh\text{-}\gamma^{del/del}$ single mutants, died within hours of birth. They displayed a tremor and decrements in reflex action and voluntary movement and did not feed or right themselves. Their neurological defects were similar to, but less severe than, those in $Pcdh\text{-}\gamma^{del/del}$ mice.

To assess synapse number and composition, we labeled spinal cords of the double mutants with antibodies to the synaptic vesicle proteins, synaptophysin and SV2, which label all presynaptic terminals; to PSD-95, which stains glutamatergic postsynaptic sites; and to gephyrin and glycine receptors, which stain inhibitory postsynaptic sites. In all cases, synapses were present, but their density was lower in $Pcdh\text{-}\gamma^{del/del}$;$Bax^{-/-}$ mice than in $Bax^{-/-}$ or $Bax^{+/-}$ controls (Fig. 2 and data not shown). Postsynaptic markers were used for quantitative analysis, because their appearance was more punctate than that of the presynaptic markers. The density of excitatory (PSD-95-positive) and inhibitory (glycine receptor- or gephyrin-positive) synapses did not differ significantly between control and $Bax^{-/-}$ mice, but was decreased 30–50% in double mutants (Fig. 2*B*). This decrease was similar to, although not quite as severe as, that seen in $Pcdh\text{-}\gamma^{del/del}$ single mutants (Fig. 2*B*). Thus, even when the deleterious effect of *Pcdh-γ* deletion on neuronal survival is abrogated, synaptic defects persist.

Synaptic Defects in γ-Pcdh Hypomorphs. A potential problem in using $Bax^{-/-}$ mice to rescue neurons is that some steps in apoptotic pathways proceed in the absence of Bax (31), so the rescued neurons could be abnormally susceptible to loss of γ-Pcdhs. A way to circumvent this limitation was provided by an allele initially generated for another purpose. In this allele, a cassette containing an internal ribosome entry site and a reporter gene was inserted into the last coding exon of the *Pcdh-γ* locus, resulting in the deletion of 57 aa at the carboxyl terminus of all *Pcdh-γ* isoforms (Fig. 3*A*). Northern analysis of tissue from the resulting truncation ($Pcdh\text{-}\gamma^{tr/tr}$) mutants confirmed that the 3′ end of the *Pcdh-γ* mRNA had been replaced by sequences in the inserted cassette (Fig. 3*B*), although expression of the reporter protein was only barely detectable in embryos and neonates (data not shown).

To characterize the protein product of the $Pcdh\text{-}\gamma^{tr/tr}$ allele, we immunoblotted brain lysates with a polyclonal antiserum to peptides encoded by the *Pcdh-γ* common exons. $Pcdh\text{-}\gamma^{tr/tr}$ and control brains both contained immunoreactive proteins of appropriate mass as judged by using recombinant *Pcdh-γ* as a standard (Fig. 3*C*). Heterogeneity in mass is likely to reflect differences in glycosylation among isoforms. Antibody specificity was demonstrated by the absence of immunoreactive material in $Pcdh\text{-}\gamma^{del/del}$ brain (Fig. 3*C*).

Levels of *Pcdh-γ* protein were several-fold lower in $Pcdh\text{-}\gamma^{tr/tr}$ brains than in controls. One possible confound was that the antiserum we used may have recognized epitopes in the carboxyl-terminal segment that is deleted in this mutant, in which case decreased immunoreactivity would reflect loss of epitopes rather than decreased protein levels. To test this possibility, we transiently transfected COS cells with constructs encoding a full-length or a C-terminally truncated *Pcdh-γ* isoform fused to GFP (see *Materials and Methods*). Proteins from these transfectants were blotted and probed with anti-GFP and anti-Pcdh-γ antisera. The ratio of GFP-to-Pcdh-γ immunoreactivity was similar for the two recombinant proteins (Fig. 3*D*), showing that predominant epitopes recognized by the anti-Pcdh-γ antiserum were retained in the truncated proteins. We conclude that the $Pcdh\text{-}\gamma^{tr}$ allele produces Pcdh-γ protein that is reduced both in size and amount compared with that in WT mice. The reduced levels might reflect defects in production or stability of mRNA or protein.

$Pcdh\text{-}\gamma^{tr/tr}$ mice, like $Pcdh\text{-}\gamma^{del/del}$;$Bax^{-/-}$ and $Pcdh\text{-}\gamma^{del/del}$ mice, died within several hours of birth, with movement defects more similar in severity to those in $Pcdh\text{-}\gamma^{del/del}$;$Bax^{-/-}$ double mutants than to those in $Pcdh\text{-}\gamma^{del/del}$ single mutants. The histological organization of the spinal cord in $Pcdh\text{-}\gamma^{tr/tr}$ mice also resembled that in $Pcdh\text{-}\gamma^{del/del}$;$Bax^{-/-}$ mice in that its size, shape, and neuronal density were normal (Fig. 4 *A*, *B*, and *D*) and levels of apoptosis were low (Fig. 4*C*). However, the density of excitatory and inhibitory synapses was decreased by ≈40–50% compared to controls (Fig. 4 *E* and *F* and data not shown). Thus,

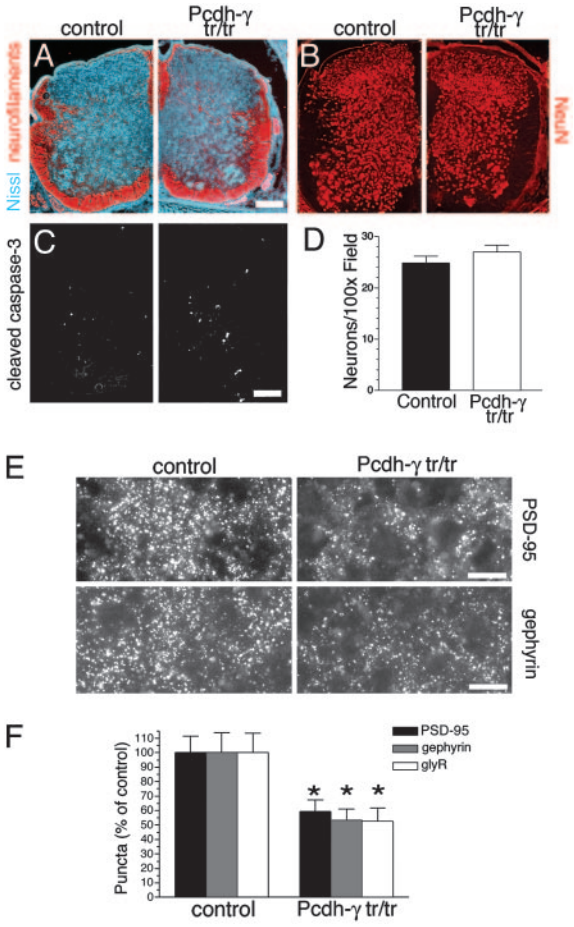

Fig. 4. Reduced synaptic density in the absence of neurodegeneration in $Pcdh\text{-}\gamma^{tr/tr}$ spinal cord. (*A–C*) Immunostained sections through the spinal cords of neonatal control and $Pcdh\text{-}\gamma^{tr/tr}$ mice. $Pcdh\text{-}\gamma^{tr/tr}$ spinal cords are morphologically normal and exhibit little or no evidence of neurodegeneration (*A*), neuronal loss (*B*, quantitation in *D*), or apoptosis (*C*). However, $Pcdh\text{-}\gamma^{tr/tr}$ spinal cords exhibit significant reductions in the density of both excitatory and inhibitory synapses [micrographs in *E* (stained as in Fig. 2), quantitation in *F*]. (Bars: 100 μm, *A–C*; 12 μm, *E*.) Bars in *D* and *F* show mean ± SEM of 21 microscope fields from three animals per genotype. *, $P < 0.0001$, compared with controls.

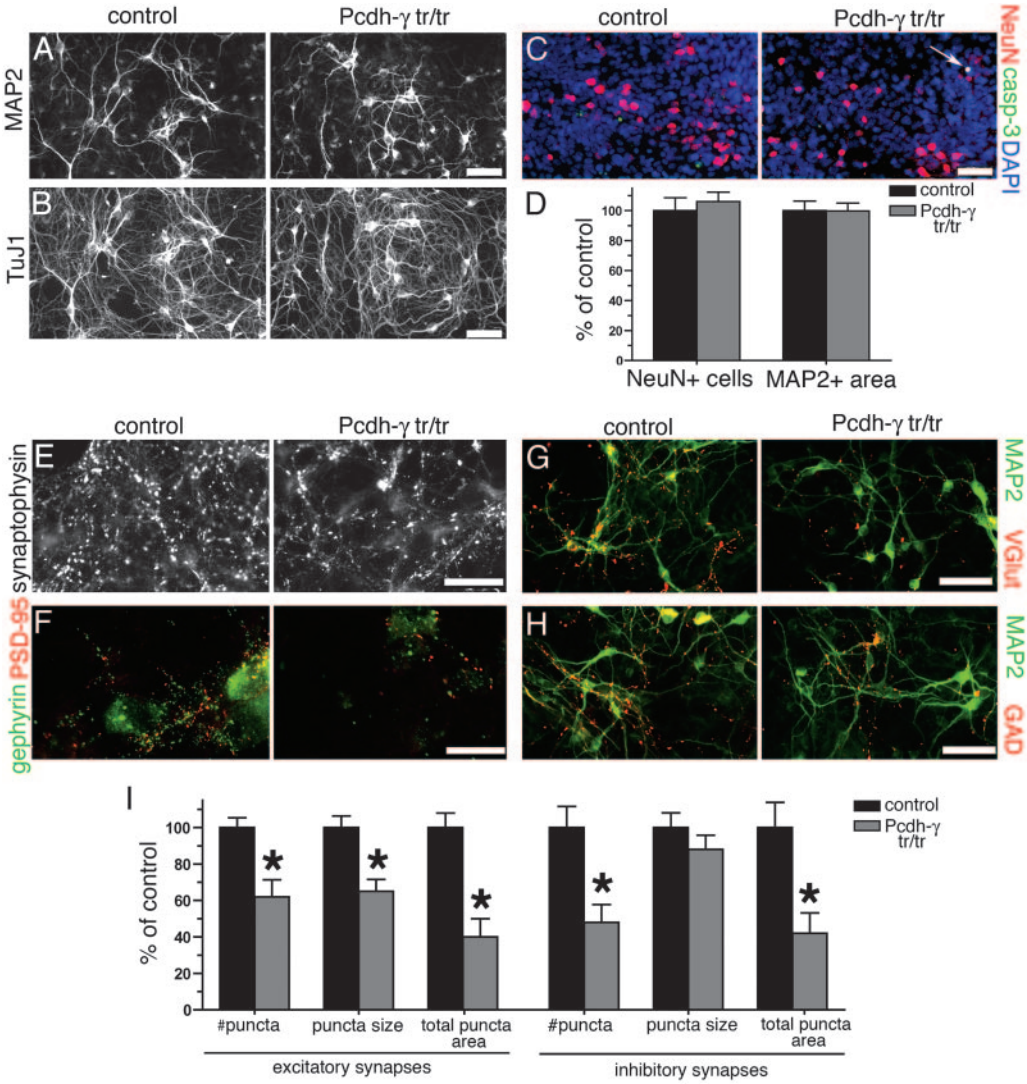

Fig. 5. Normal differentiation but abnormal synaptic development in cultured *Pcdh-*$\gamma^{tr/tr}$ spinal interneurons. Cultures were fixed and stained at 9 days *in vitro*. (*A–C*) Mutant neurons differentiate normally *in vitro* as *in vivo*, as assessed by MAP2 (*A*), class III β-tubulin (*B*), and NeuN (*C*) expression. Apoptotic mutant neurons are only rarely observed (*C*, arrow); most cleaved caspase-3+ cells in the cultures are glia. (*D*) Neither neuronal density (NeuN+) nor somato-dendritic area (MAP2+) differed between control and *Pcdh-*$\gamma^{tr/tr}$ cultures. (*E–H*) Synapses formed in mutant cultures, as detected with antibodies to presynaptic terminals [synaptophysin for all terminals (*E*); VGlut for excitatory terminals (*G*); GAD for inhibitory terminals (*H*)] and to PSDs [PSD-95 for excitatory and gephyrin for inhibitory (*F*)]. (Bars: 30 μm in *A–C*, *G*, and *H*; 10 μm in *E* and *F*.) (*I*) The number of excitatory (VGlut+) and inhibitory (GAD+) terminals, and the average size of excitatory terminals, are decreased in mutants. Bars in *I* show mean ± SEM for 24–30 microscope fields obtained from three separate cultures including five control and four mutant embryos. Number of puncta and puncta area are shown normalized to MAP2+ area [which did not differ between genotypes (*D*)]. *, $P < 0.001$, compared with controls.

the *Pcdh-*γ protein that persists in the *Pcdh-*$\gamma^{tr/tr}$ mice is sufficient for neuronal survival, but insufficient to support normal synaptic development.

Synaptic Defects in Neurons Cultured from *Pcdh-*$\gamma^{tr/tr}$ Mice. As a third approach to analyzing the role of *Pcdh-*γ in synaptic development, we cultured spinal neurons from *Pcdh-*$\gamma^{tr/tr}$ mice (see *Materials and Methods*). Immunofluoresence confirmed a reduction in *Pcdh-*γ protein levels in *Pcdh-*$\gamma^{tr/tr}$ cultures, similar to that observed in intact brain tissue (data not shown). In both *Pcdh-*$\gamma^{tr/tr}$ and control cultures, neurons differentiated (expressed NeuN), extended tubulin-rich processes (TuJ1-positive), some of which differentiated into dendrites (MAP2-positive), and exhibited little apoptosis (as assayed with anti-activated caspase 3) (Fig. 5 *A–C*). In the serum-containing medium we used, many neurons survived for at least 12 days.

Quantitative analysis revealed no significant differences between *Pcdh-*$\gamma^{tr/tr}$ and control cultures in neuron number or dendritic area (Fig. 5*D*). However, the number of synapses was reduced in *Pcdh-*$\gamma^{tr/tr}$ cultures (Fig. 5 *E–I*), as assayed with antibodies against a panel of presynaptic and postsynaptic proteins: synaptophysin, present at all terminals; VGlut, a marker of excitatory nerve terminals; GAD, a marker of inhibitory nerve terminals; and PSD-95 and gephyrin, markers of excitatory and inhibitory PSDs, respectively. Both excitatory and inhibitory synaptic populations were significantly affected. Synaptic puncta were decreased in average size as well as in number in the mutant cultures, although the difference in size was statistically significant only for excitatory synapses (Fig. 5*I*). Thus, *in vitro* as *in vivo*, synaptic development is perturbed in *Pcdh-*$\gamma^{tr/tr}$ neurons, despite seemingly normal neuronal differentiation and survival.

To assess the physiological consequences of *Pcdh-*γ deficiency,

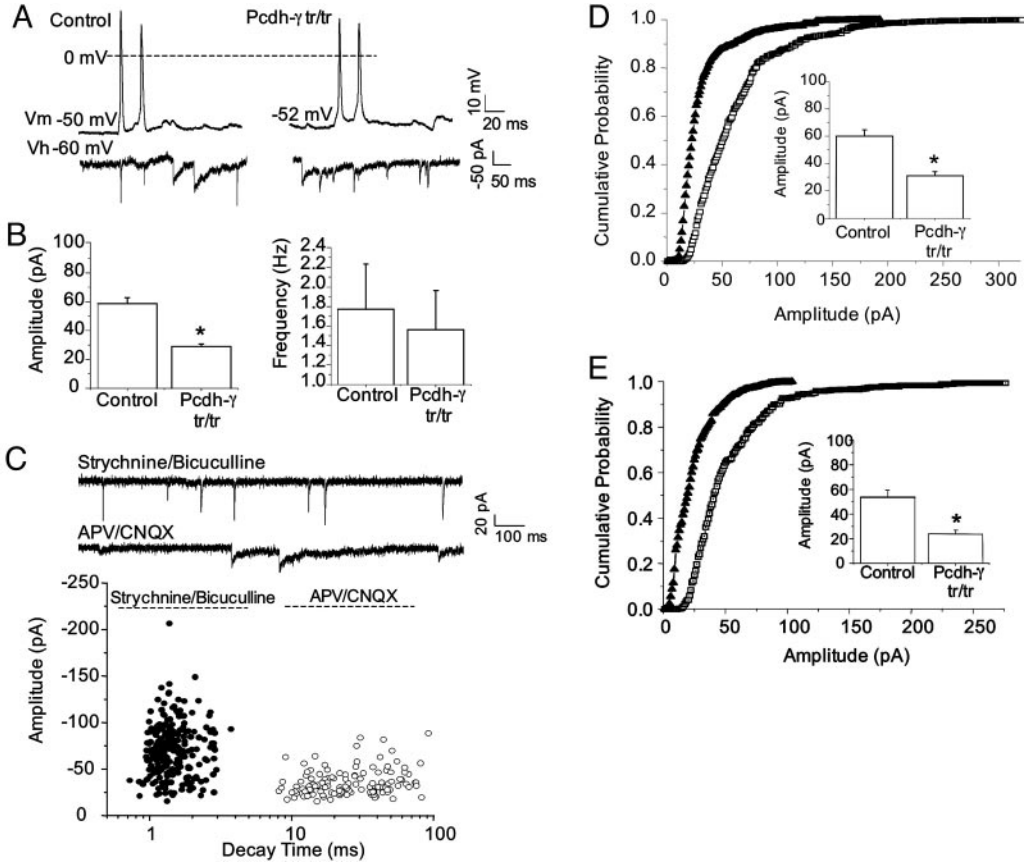

Fig. 6. Reduced synaptic current amplitude in *Pcdh*-$\gamma^{tr/tr}$ neurons. (*A*) Action potentials (*Upper*) and spontaneous synaptic events (*Lower*) were recorded from control (*Left*) and *Pcdh*-$\gamma^{tr/tr}$ (*Right*) neurons. Vm, membrane resting potential; Vh, holding potential. (*B*) Mean synaptic amplitude (*Left*) was significantly lower in *Pcdh*-$\gamma^{tr/tr}$ (29 ± 2 pA) than in control (58 ± 5 pA) neurons. *, $P < 0.05$; $n = 30–39$ cells per genotype. The mean synaptic frequency (*Right*) was similar in control (1.78 ± 0.45 Hz) and *Pcdh*-$\gamma^{tr/tr}$ (1.57 ± 0.39) neurons. (*C*) Pharmacological isolation of spontaneous excitatory (upper trace) and inhibitory (lower trace) synaptic events. Note the fast (<5 ms) and slow (>10 ms) decay times of the excitatory (●) and inhibitory (○) synaptic events respectively. $n = 7–8$ cells per pharmacological condition. CNQX, 6-cyano-7-nitroquinoxaline-2,3-dione; APV, 2-amino-5-phosphonovaleric acid. (*D* and *E*) Cumulative probability histograms demonstrate the reduction in excitatory (*D*) and inhibitory (*E*) synaptic amplitudes in *Pcdh*-$\gamma^{tr/tr}$ neurons. ▲, Pchd$^{tr/tr}$; □, control. (*Insets*) The mean amplitudes for control and *Pcdh*-$\gamma^{tr/tr}$ excitatory (*D*) and inhibitory (*E*) synaptic events are shown. $n = 15–20$ neurons each genotype. *, $P < 0.05$.

we recorded spontaneous synaptic currents from neurons in *Pcdh*-$\gamma^{tr/tr}$ and control cultures. Depolarization elicited action potentials from both mutant and control neurons (Fig. 6*A Upper*). Neither membrane potential (V_M) nor action potential threshold differed significantly between genotypes (V_M −54 ± 2 mV and −57 ± 3 mV in *Pcdh*-$\gamma^{tr/tr}$ and controls, respectively; threshold −43 ± 6 mV and −40 ± 3 mV in *Pcdh*-$\gamma^{tr/tr}$ and controls, respectively; $n = 4$ cells per genotype). Moreover, recordings in voltage clamp mode revealed spontaneous synaptic currents in both mutant and control neurons (Fig. 6*A Lower*). Their frequency was lower in mutant than in control neurons, but this difference was not statistically significant (Fig. 6*B Right*). However, the mean amplitude of the synaptic currents recorded from mutant neurons was ~50% lower than those in controls (Fig. 6*B Left*). This result suggests that γ-Pcdhs are required for the development and/or function of synapses.

To ask whether *Pcdh*-γ affects excitatory or inhibitory synapses, we took account of the fact that decay times of excitatory (glutamatergic) currents recorded from cultured mammalian central neurons are considerably faster than those of inhibitory (GABAergic and glycinergic) currents (32, 33). Pharmacological tests confirmed this distinction in our cultures: excitatory currents, isolated by addition of GABAergic and glycinergic blockers (200 nM strychnine and 2 μM bicuculline), had decay times of 0.5–4 ms, whereas inhibitory currents, isolated by addition of glutamatergic blockers (2 mM 6-cyano-7-nitroquinoxaline-2,3-dione and 20 μM 2-amino-5-phosphonovaleric acid), had decay times of 7–100 ms (Fig. 6*C*). Using decay time as a criterion, we found that both excitatory synaptic currents (<8 ms decay time; Fig. 6*D*) and inhibitory synaptic currents (>10 ms decay time; Fig. 6*E*) were significantly smaller in mutants than in controls. Thus, truncation and/or reduced expression of γ-Pcdhs leads both to fewer synapses and reduced synaptic activity at those synapses that are present.

Discussion

Our initial studies of mice lacking γ-Pcdhs established the importance of these molecules for the development of the nervous system, but we could not tell whether the observed synaptic deficits were a direct effect of *Pcdh*-γ mutation or secondary to interneuron loss (17). Here, we used two additional mutants, *Bax*$^{-/-}$ and *Pcdh*-$\gamma^{tr/tr}$, to test the role of γ-Pcdhs in synaptic development.

Neurodegeneration was minimal but synaptic defects were dramatic in spinal cords of both *Pcdh*-$\gamma^{del/del}$;*Bax*$^{-/-}$ double mutants and *Pcdh*-$\gamma^{tr/tr}$ hypomorphs. Similarly, *Pcdh*-$\gamma^{tr/tr}$ interneurons survived and differentiated *in vitro* but exhibited fewer and weaker synapses than did control interneurons. The fact that both the double mutants and the hypomorphs exhibit sensorimotor defects and die at birth suggests that the synaptic defects are biologically as well as statistically significant.

It remains to be determined which stages of synaptic development are regulated by γ-Pcdhs. Possibilities include the initial formation of synaptic contacts, their maturation into fully functional synapses, and the maintenance of their structural or physiological integrity. One hint comes from our observations that synaptic puncta are decreased in size as well as number in mutant neurons *in vitro*, and that mutant synaptic currents are reduced in amplitude rather than frequency. These results suggest that γ-Pcdhs affect synaptic maturation or maintenance. The decreased number of synaptic puncta in mutants *in vivo* and *in vitro* suggests an additional effect on the initial steps of synaptogenesis, but could also reflect an inability to detect the smallest, presumably least mature, synapses. That is, small synaptic puncta are difficult to distinguish from background fluorescence, so that a decrease in average size would be conflated with a decrease in number.

Whatever the stage at which they act, γ-Pcdhs might be required either for generic synaptic functions or synaptic specificity, as suggested by the diversity of their extracellular domains. Either role could result in decreased synapse number or size, if one imagines that synapses formed between "inappropriate" partners are smaller, weaker, or less stable than those found in "appropriate" circuits. Indeed, such defects have been observed in several cases in which neurons formed synapses on inappropriate targets either transiently during development or because of experimental manipulations (34–37). One way to distinguish these possibilities would be to ask whether misexpression of one or a few *Pcdh-γ* isoforms affects patterns of connectivity. The demonstration that Pcdhs play separate roles in neuronal survival and synaptic development makes these issues important to address, and our genetic methods for separating trophic from synaptic effects of Pcdhs make the appropriate experiments possible.

We thank Dr. Andreas Burkhalter (Washington University) for use of his patch-clamping rig and Dr. Monica Carrasco for helpful advice on spinal neuron cultures. This work was supported by a National Eye Institute/National Institutes of Health postdoctoral fellowship (to J.A.W.) and grants from the National Institute of Neurological Disorders and Stroke/National Institutes of Health (to J.R.S.).

1. Yamagata, M., Sanes, J. R. & Weiner, J. A. (2003) *Curr. Opin. Cell Biol.* **15,** 621–632.
2. Scheiffele, P. (2003) *Annu. Rev. Neurosci.* **26,** 486–508.
3. Washbourne, P., Ditayetev, A., Scheiffele, P., Biederer, T., Weiner, J. A., Christopherson, K. S. & El-Husseini, A. (2004) *J. Neurosci.* **24,** 9244–9249.
4. Takai, Y., Shimuzu, K. & Ohtsuka, T. (2003) *Curr. Opin. Neurobiol.* **13,** 520–526.
5. Yamagata, M., Weiner, J. A. & Sanes, J. R. (2002) *Cell* **110,** 649–660.
6. Shen, K. & Bargmann, C. I. (2003) *Cell* **112,** 619–630.
7. Shen, K., Fetter, R. D. & Bargmann, C. I. (2004) *Cell* **116,** 869–881.
8. Wojtowicz, W. M., Flanagan, J. J., Millard, S. S., Zipursky, S. L. & Clemens, J. C. (2004) *Cell* **118,** 619–633.
9. Zhan, X. L., Clemens, J. C., Neves, G., Hattori, D., Flanagan, J. J., Hummel, T., Vasconcelos, M. L., Chess, A. & Zipursky, S. L. (2004) *Neuron* **43,** 673–686.
10. Wu, Q. & Maniatis, T. (1999) *Cell* **97,** 779–790.
11. Wu, Q., Zhang, T., Cheng, J. F., Kim, Y., Grimwood, J., Schmutz, J., Dickson, M., Noonan, J. P., Zhang, M. Q., Myers, R. M. & Maniatis, T. (2001) *Genome Res.* **11,** 389–404.
12. Obata, S., Sago, H., Mori, N., Davidson, M., St. John, T. & Suzuki, S. T. (1998) *Cell Adhes. Commun.* **6,** 323–333.
13. Sugino, H., Hamada, S., Yasuda, R., Tuji, A., Matsuda, Y., Fujita, M. & Yagi, T. (2000) *Genomics* **63,** 75–87.
14. Wang, X., Su, H. & Bradley, A. (2002) *Genes Dev.* **16,** 1890–1905.
15. Tasic, B., Nabholz, C. E., Baldwin, K. K., Kim, Y., Rueckert, E. H., Ribich, S. A., Cramer, P., Wu, Q., Axel, R. & Maniatis, T. (2002) *Mol. Cell* **10,** 21–33.
16. Kohmura, N., Senzaki, K., Hamada, S., Kai, N., Yasuda, R., Watanabe, M., Ishii, H., Yasuda, M., Mishina, M. & Yagi, T. (1998) *Neuron* **20,** 1137–1151.
17. Wang, X., Weiner, J. A., Levi, S., Craig, A. M., Bradley, A. & Sanes, J. R. (2002) *Neuron* **36,** 843–854.
18. Phillips, G. R., Tanaka, H., Frank, M., Elste, A., Fidler, L., Benson, D. L. & Colman, D. R. (2003) *J. Neurosci.* **23,** 5096–5104.
19. Blank, M., Triana-Baltzer, G. B., Richards, C. S. & Berg, D. K. (2004) *Mol. Cell Neurosci.* **26,** 530–543.
20. Shapiro, L. & Colman, D. R. (1999) *Neuron* **23,** 427–430.
21. Hamada, S. & Yagi, T. (2001) *Neurosci. Res.* **41,** 207–215.
22. Benson, D. L., Colman, D. R. & Huntley, G. W. (2001) *Nat. Rev. Neurosci.* **2,** 899–909.
23. Knudson, C. M., Tung, K. S., Tourtellotte, W. G., Brown, G. A. & Korsmeyer, S. J. (1995) *Science* **270,** 96–99.
24. Deckwerth, T. L., Elliott, J. L., Knudson, C. M., Johnson, E. M., Jr., Snider, W. D. & Korsmeyer, S. J. (1996) *Neuron* **17,** 401–411.
25. White, F. A., Keller-Peck, C. R., Knudson, C. M., Korsmeyer, S. J. & Snider, W. D. (1998) *J. Neurosci.* **18,** 1428–1439.
26. Pequignot, M. O., Provost, A. C., Salle, S., Taupin, P., Sainton, K. M., Marchant, D., Martinou, J. C., Ameisen, J. C., Jais, J. P. & Abitbol, M. (2003) *Dev. Dyn.* **228,** 231–238.
27. Patel, T. D., Jackman, A., Rice, F. L., Kucera, J. & Snider, W. D. (2000) *Neuron* **25,** 345–357.
28. Misgeld, T., Burgess, R. W., Lewis, R. M., Cunningham, J. M., Lichtman, J. W. & Sanes, J. R. (2002) *Neuron* **36,** 635–648.
29. Ransom, B. R., Neale, E., Henkart, M., Bullock, P. N. & Nelson, P. G. (1977) *J. Neurophysiol.* **40,** 1132–1150.
30. Van Zundert, B., Alvarez, F. J., Tapia, J. C., Yeh, H. H., Diaz, E. & Aguayo, L. G. (2004) *J. Neurophysiol.* **91,** 1036–1049.
31. Miller, T. M., Moulder, K. L., Knudson, C. M., Creedon, D. J., Deshmukh, M., Korsmeyer, S. J. & Johnson, E. M., Jr. (1997) *J. Cell Biol.* **139,** 205–217.
32. Gao, B. X., Cheng, G. & Ziskind-Conhaim, L. (1998) *J. Neurophysiol.* **79,** 2277–2287.
33. Galante, M., Nistri, A. & Ballerini, L. (2000) *J. Physiol. (London)* **523,** 639–651.
34. Purves, D., Thompson, W. & Yip, J. W. (1981) *J. Physiol. (London)* **313,** 49–63.
35. Wigston, D. J. & Sanes, J. R. (1982) *Nature* **299,** 464–467.
36. Butler, J., Cauwenbergs, P. & Cosmos, E. (1986) *J. Embryol. Exp. Morphol.* **95,** 147–168.
37. Seebach, B. S. & Ziskind-Conhaim, L. (1994) *J. Neurosci.* **14,** 4520–4528.